

Robust Control H_∞ Fuzzy of a Doubly Fed Induction Generator Integrated to Wind Power System

Lakhdar Saihi^{1,2*}, Brahim Berbaoui², Hachemi Glaoui¹

1- Department of Electrical and Computer Engineering, University of Tahri Mohamed Bechar, Bp 417, Algeria.

Email: saihi_lakhdar@urerms.dz (Corresponding author), Email: glaouih@yahoo.fr

2-Unité de Recherche en Energies Renouvelables en Milieu Saharien URERMS,

Centre de Développement des Energies Renouvelables CDER, 01000, Adrar, Alegria.

Email: berbaoui.brahim@gmail.com

Received: May 2109

Revised: August 2019

Accepted: October 2019

ABSTRACT:

This paper proposes a H_∞ Fuzzy robust controller for Doubly Fed Induction Generator (DFIG) based wind turbines. The power exchange between the machine stator and the grid is carried out by acting on the rotor via a bidirectional converter. The control objective is to regulate the stator active and reactive power generated from the DFIG by means of two kinds of controllers named H_∞ PI and H_∞ Fuzzy. Comparison study between the proposed controllers considering reference tracking and robustness to parameter variations is discussed. Simulation results illustrate the effectiveness of the H_∞ Fuzzy controller compared with the other one for time-varying reference tracking and parameters variations, which improves quality and quantity of generated power.

KEYWORDS: DFIG Generator, Wind Turbine, Robust Control, H_∞ Fuzzy Controller, Weighing Function.

1. INTRODUCTION

Recently, the importance of wind power generation has led people to conduct extensive researches. These research objectives are to improve the efficiency and quality of the wind system and the produced power respectively, by selecting an optimal system architecture and developing a robust control able to compensate the effects of the parameter variations and the external disturbances [1].

Most of the wind turbines installed today are equipped with a Doubly Fed Induction Generator (DFIG). This configuration is adopted for variable energy conversion. The DFIG rotor winding is fed by two static converters separated by a continuous bus. This is the most known configuration in recent years, because it has many technical and economic advantages, especially when it is compared with the other configurations based on cage asynchronous machine or synchronous machine. This configuration allows to operate over a wide range of wind speeds, and to get the maximum power from variable wind speed [1], [2], [7].

In the industrial wind system, the conventional controllers are widely used such as Proportion-Integral (PI), Proportion-Integral-Derivative (PID) [5], [14]; due to their simple configuration. These controllers are highly depended on control system parameters and they do not guarantee the system stability. Control structures based on these conventional controllers are not able to

ensure the desired performances. For context, the concept of robustness appears as an essential characteristic that must be taken into account in the synthesis of controllers [2], [3].

A robust control law aims to obtain acceptable operation of a real system under different conditions and modes of use, ensuring the stable dynamics of the controlled process. In this sense, advanced controllers also called robust controllers are proposed as alternative method to solve the control problem mentioned above. One of them is H_∞ approach where the automation engineer introduces the mathematical model of the controlled system with structured or unstructured uncertainties in additive or multiplicative form [8]. An optimization algorithm is then mounted seeking to maximize the stability of the closed-loop system taking into account these uncertainties. In addition, performance objectives can be added as an objective of the optimization algorithm [1].

Because of the disturbances, the development of robust controller is very important. Fuzzy logic control is one of the important branches of strategies artificial intelligence that is able to reproduce human reasoning and occupies a large place in modern research fields [13]. This technique becomes very dominant in several industrial fields. The fuzzy logic setting does not deal with a well-defined mathematical relationship, but uses inferences with multiple rules; based on linguistic

variables. Thus, it is possible to take into account the experiences acquired by the technical process operators [14]. The integration of fuzzy logic into the H_∞ approach presents a strong solution to ensure optimal regulation that meets the requirements of the user even in a difficult and variable environment [13].

Marouane E, Hassane M, Chafik E. [2] have proposed an algorithm which could the nonlinear Backstepping approach while the field orientation is applied to control the DFIG. They have found that this combining presents the performances in terms of set point tracking, stability, but does not eliminate oscillations completely. Doumi M, Aissaoui A. [3] have examined the decoupling control of active and reactive powers by Nonlinear Backstepping control of a DFIG which shows superiority over PI during the robustness, but this method had a slow response time.

Swagat P, Swati S. [5] have used stator-flux oriented vector control scheme which is used in machine-side converter by which decouple control of active and reactive of DFIG is achieved, but this control had oscillations, exceeding, and the decoupling is not fully maintained.

Sebastian K, Yusuke M. [6] proposed a new H_∞ robust control strategy for DFIG to improve transient stability during uncertainties and grid faults, the performance of the proposed H_∞ control approach is more effective than that of the conventional PI control, but it can also be extended to H_∞ design problems for decentralized control systems and descriptor systems. Wang, Y; Wu, Q. [7] proposed an H_∞ robust controller which was designed for the DFIG rotor current regulation in order to improve the robustness and harmonic suppression performance subject to grid voltage distortions and generator parameter perturbation.

The aim of the work performed by Hamane B, Benganem M. [16] is to apply and compare the dynamic performances of two types of controllers (namely, classical PI and Fuzzy-PI) for the WECS in terms of tracking and robustness with respect to the wind fluctuation as well as the impact on the quality of the energy produced. The performed work by Marouane E. [17] deals with the vector control based on fuzzy logic of active and reactive power of DFIG. For a comparative study, the independent control of active and reactive power is ensured in the first step by conventional controllers (PI) and the second step by the fuzzy controller. In addition, the performance and robustness are analyzed.

Zerzouri et al. [18] tried to improve the performance of WECS based DFIG, they decoupled the active and reactive power of the stator and they used a single PI in each control loop, but the oscillations were remained apparent.

The focus of this paper is on implementation of H_∞

controller combined with fuzzy logic control for the adjustment of active and reactive power which is organized as following; the wind turbine characteristics are described in section II, modeling of the proposed system is introduced in section III, the H_∞ approach and fuzzy logic controller are synthesized in section IV, simulation result is presented in section V, finally conclusions are stated.

2. MODELING OF THE WIND POWER SYSTEM

Fig. 1 shows the DFIG based wind turbine configuration. The DFIG stator is directly connected to the grid and the rotor is linked to the grid through a back-to-back converter based IGBT's (In-Gate Bipolar Transistor) controlled by Pulse Width Modulation (PWM). Back-to-back converter consists of two voltage converters (rotor side converter (RSC) and the grid side converter (GSC)) with a DC bus in common [1], [2].

We are interested in controlling the active and reactive powers of the DFIG through the RSC converter.

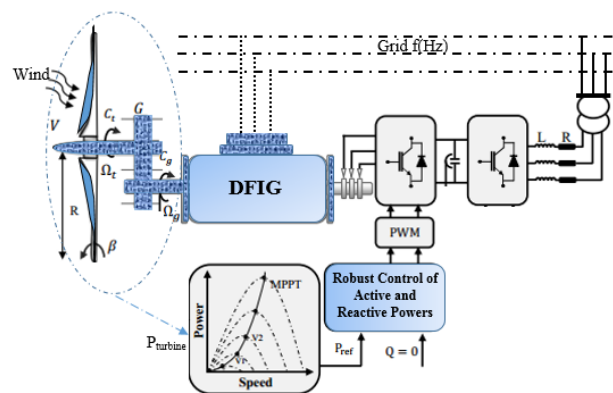


Fig. 1. DFIG based wind turbine while system.

2.1. Wind Turbine Modelling

It is assumed that the velocity V of the wind passing through a surface S is constant. The aerodynamic power P_{aer} is given by the expression (1) [2], [4]:

$$P_{aer} = \frac{1}{2} \rho A v^3 C_p(\lambda, \beta) \quad (1)$$

The power P_T of the turbine according to Betz's theory is:

$$P_T = \frac{1}{2} \rho A v^3 C_p(\lambda, \beta) \quad (2)$$

Where, ρ (1.225 kg.m-3) is the air density, $A = \pi R_T^2$ is the turbine blade sweep area (m²), with R_T (m) is the turbine radius, v (m.s-1) is the wind speed and $C_p(\lambda, \beta)$ is the power coefficient, which represents the

aerodynamic efficiency of the turbine and also depends on the tip speed ratio λ and the blade pitch angle β , as described as :

$$C_p(\lambda, \beta) = \frac{1}{2} \left(\frac{116}{\lambda_i} - 0.4\beta - 5 \right) e^{-\left(\frac{21}{\lambda_i}\right)} \quad (3)$$

$$\lambda_i = \left(\frac{1}{\lambda + 0.08\beta} - \frac{0.035}{\beta^3 + 1} \right) \quad (4)$$

A plot of the variation of this coefficient as a function of the specific speed λ for different values of the blade orientation angle β , (Fig. 2), allows to have the maximum point of this coefficient $C_{pmax}(\lambda, \beta) = 0.44$, which corresponds to the optimal values $\lambda_{opt} = 10.54$ and $\beta = 2^\circ$, with these values, the wind turbine will be operated to extract the maximum power form wind [3], [5].

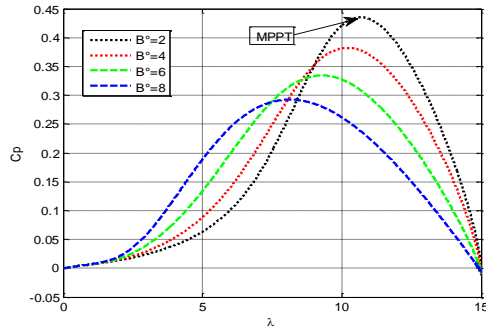


Fig. 2. Power coefficient.

To describe the wind turbine operation speed, using the reduced (specific) speed λ , which is the ratio of the linear speed at the end of the turbine blade brought back to the wind speed:

$$\lambda = \frac{R_T \Omega_t}{v} \quad (5)$$

The speed of the turbine is known, the torque of the turbine is determined as follows [2], [3], [4]:

$$T_t = \frac{1}{2} \rho \pi R_T^3 v^2 C_p(\lambda, \beta) \quad (6)$$

2.2. Mechanical Shaft Modeling

The mechanical system is represented by the following equation [3]:

$$J_T \frac{d\Omega_t}{dt} = T_t - T_{em} - f\Omega_t \quad (7)$$

Where, J_T (kg.m²) is the total inertia which appears on the shaft of the generator, T_t (N.m) is the mechanical torque, T_{em} (N.m) is the electromagnetic torque applied to the DFIG rotor, and f (N.m.s.rad⁻¹) is a viscous friction coefficient.

2.3. DFIG Modeling

The DFIG is a classic machine where its rotor is accessible and identical to the stator. Therefore, it has the same model as the cage asynchronous machine, with the exception of rotor voltages which are not zero [3], [4]. The equations of the electrical voltages that govern the DFIG are:

$$\begin{cases} v_{ds} = R_s \cdot i_{ds} + \frac{d\varphi_{ds}}{dt} - \omega_s \cdot \varphi_{qs} \\ v_{qs} = R_s \cdot i_{qs} + \frac{d\varphi_{qs}}{dt} + \omega_s \cdot \varphi_{ds} \\ v_{dr} = R_r \cdot i_{dr} + \frac{d\varphi_{dr}}{dt} - (\omega_s - \omega_r) \cdot \varphi_{qr} \\ v_{qr} = R_r \cdot i_{qr} + \frac{d\varphi_{qr}}{dt} - (\omega_s - \omega_r) \cdot \varphi_{dr} \end{cases} \quad (8)$$

The magnetic flux equations that govern DFIG are:

$$\begin{cases} \varphi_{dr} = l_s \cdot i_{ds} + l_m \cdot i_{dr} \\ \varphi_{qs} = l_s \cdot i_{qs} + l_m \cdot i_{qr} \\ \varphi_{dr} = l_r \cdot i_{dr} + l_m \cdot i_{ds} \\ \varphi_{qr} = l_r \cdot i_{qr} + l_m \cdot i_{qs} \end{cases} \quad (9)$$

Where, l_s and l_r are respectively the stator and the rotor inductances, l_m is the mutual inductance, i_d and i_q are the equivalent current of d and q axis; R_s , R_r are respectively the stator and the rotor resistance; Ω_t is the electrical angular speed, $\Omega_t = p \omega$, p is the number of pole pairs; φ_q , φ_d are respectively direct and quadrature flux; v_d and v_q are direct and quadratic voltages respectively.

The electromagnetic torque expression is given as:

$$T_{em} = p \cdot \frac{l_m}{l_s} (i_{ds} \cdot i_{qr} - i_{dr} \cdot i_{qs}) \quad (10)$$

The active (P_s) and reactive (Q_s) stator power are [3], [4]:

$$\begin{cases} P_s = (v_{ds} \cdot i_{ds} + v_{qs} \cdot i_{qs}) \\ Q_s = (v_{qs} \cdot i_{ds} - v_{ds} \cdot i_{qs}) \end{cases} \quad (11)$$

Using Field Oriented Control (FOC) strategy [3], [18], the DFIG control scheme is given as [6], [18]:

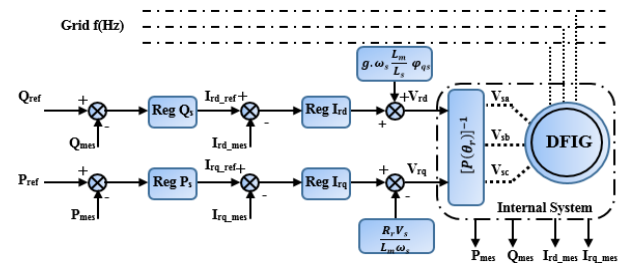


Fig. 3. Global control structure of the wind generator with DFIG.

According to Fig. 3, there are four regulators (two power regulators and two regulators for currents). We make a combination between the H_∞ controller and the fuzzy logic controller on each axis d and q , where the H_∞ is used to control the DFIG stator powers and the fuzzy logic controller is installed to control the DFIG rotor currents.

3. ROBUST H_∞ CONTROL APPROACH

The robustness of enslaved systems is important. Industrial applications are submitted to external disturbances and measurement noise, in addition, the mathematical model of the controlled system does not always describe the full system dynamics such as parametric uncertainties and unmodeled dynamics. The robust control H_∞ is an interesting solution for system uncertainties [8], [12].

3.1. General Control Configuration with Uncertainty

The standard configuration of H_∞ controller $K(s)$ with the plant $P_M(s)$ and the uncertainties W_n is shown in Fig. 4 [6], [7], and [10].

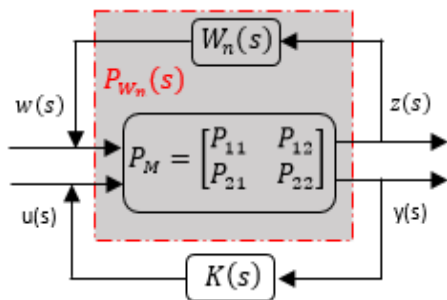


Fig. 4. General Setup of the H_∞ design problem.

$$\begin{cases} \dot{x}(t) = A \cdot x(t) + B_1(t) \cdot w(t) + B_2(t) \cdot u(t) \\ z(t) = C_1 x(t) + D_{11} \cdot w(t) + D_{12}(t) \cdot u(t) \\ y(t) = C_2 x(t) + D_{21} \cdot w(t) \end{cases} \quad (12)$$

With;

- $x(t)$: Controlled outputs vector;
- $z(t)$: Inputs vector of criterion H_∞ ;
- $y(t)$: Measured outputs vector;
- $u(t)$: Inputs vector of control;

$A, B_1, B_2, C_1, D_{11}, D_{12}, C_2, D_{21}$ Are matrices with corresponding dimensions and $W_n(s)$ is the weighting function.

The transfer matrix $P_M(s)$ describes a system comprising two inputs and two outputs with [6], [8], [9]:

$$[w] = [W_n] \cdot [z] \quad (13)$$

$$\text{with; } w = \begin{bmatrix} d_1 \\ d_2 \\ d_3 \end{bmatrix}; z = \begin{bmatrix} z_1 \\ z_2 \\ z_3 \end{bmatrix}; [W_n] = \begin{bmatrix} W_1 & 0 & 0 \\ 0 & W_2 & 0 \\ 0 & 0 & W_3 \end{bmatrix}$$

$$\begin{bmatrix} z(s) \\ y(s) \end{bmatrix} = P_M \cdot \begin{bmatrix} w(s) \\ u(s) \end{bmatrix} \quad (14)$$

If $P_M(s)$ and plant uncertainty W are combined to give $P_W(s)$, we get:

$$\begin{bmatrix} z(s) \\ y(s) \end{bmatrix} = \begin{bmatrix} W_1(s) \cdot S(s) & W_1(s) \cdot W_3(s) \cdot S(s) \cdot G(s) \\ W_2(s) \cdot K(s) \cdot S(s) & W_2(s) \cdot K(s) \cdot W_3(s) \cdot S(s) \cdot G(s) \end{bmatrix} \cdot \begin{bmatrix} w(s) \\ u(s) \end{bmatrix} \quad (15)$$

with s Laplace operator.

The standard problem of the H_∞ control is to find a $K(s)$ controller, which internally stabilizes the closed-loop as in Fig. 4, and minimizes the H_∞ norm of the transfer function from the input to the output, such that it [7], [9]:

$$\left\| \begin{bmatrix} W_1 \cdot S & W_1 \cdot W_3 \cdot S \cdot G \\ W_2 \cdot K \cdot S & W_2 \cdot K \cdot W_3 \cdot S \cdot G \end{bmatrix} \right\|_\infty < \gamma \quad (16)$$

$$\|T_{zw}\|_\infty \leq \gamma_{min} \quad \gamma > 0 \quad (17)$$

Where, T_{zw} is the transfer matrix of the input signal to the output signal, and γ is a positive constant value called optimization level.

$$z(s) = [P_{11} + P_{12} \cdot W \cdot K \cdot (I - P_{22} \cdot W)^{-1} \cdot P_{21}] \cdot w = F(P_m \cdot W) \cdot w = T_{zw} \cdot w \quad (18)$$

$$y(s) = P_W(s) \cdot u = [P_{22} + P_{21} \cdot W \cdot K \cdot (I - P_{11} \cdot W)^{-1} \cdot P_{12}] \cdot u = F(P_m \cdot W) \cdot u = T_{yu} \cdot u \quad (19)$$

From Fig. 4 we have:

$$u = K(s) \cdot y(s) \quad (20)$$

The robust controller $K(s)$ can be given by:

$$K(s) = [P_{22} + P_{21} \cdot W \cdot (I - P_{11} \cdot W)^{-1} \cdot P_{12}]^{-1} = F(SI - P_{22})^{-1} \quad (21)$$

3.2. Synthesis of the Robust Controller by the Method of Mixed Sensitivity

In this subsection, the mathematical tools necessary for the development of a robust H_∞ controller is presented.

The system augmented by the weighting functions is shown in Fig. 5 [8], [9], [11].

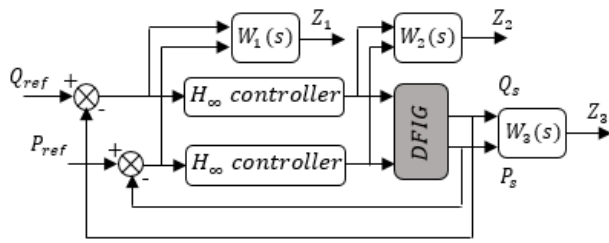


Fig. 5. Mixed Sensitivity Scheme for Robust Control Design.

To control Z_1, Z_2, Z_3 , we can write [11]:

$$Z_1 = W_1(s) \begin{bmatrix} Q_{ref} - Q \\ P_{ref} - P \end{bmatrix} \quad (22)$$

$$Z_2 = W_2(s) \cdot u(s) \quad (23)$$

$$Z_3 = W_3(s) \begin{bmatrix} Q \\ P \end{bmatrix} \quad (24)$$

with the error $E_Q = Q_{ref} - Q$ and $E_P = P_{ref} - P$ is weighted by the filter $W_1(s)$, the command u by $W_2(s)$ and the output y by $W_3(s)$. In the mixed sensitivity problem shown in Fig. 5, the computation of the robust controller $K(s)$ stabilizing the looped system passes through the choice of the weighting functions W_1, W_2 and W_3 , where it must check the condition in (16).

3.3. Weighting Functions Design

According to the stability condition in (16), it is clear that the frequency response of the functions $S(s)$, $S.K(s)$, $S.G(s)$ and $K.S.G(s)$ is constrained by a range which depends on the filters W_1, W_2, W_3 chosen. Figs. 6, 7 show the typical look you choose for ranges [8], [9], [10].

To limit the sensitivity function $S(s)$ we use $W_1(s)$ and must satisfy the condition:

$$\|W_1 \cdot S\|_\infty \leq \gamma \quad \forall \omega \in R \quad |S(j\omega)| \leq \frac{\gamma}{|W_1(j\omega)|} \quad (25)$$

$$W_1(s): \text{ written in the form: } W_1 = \frac{s/M_s + \omega_1}{s + \omega_1 \cdot \varepsilon}$$

For good choice of the weighting function $W_1(s)$, we set ε to a low value at basses frequencies. This choice gives rise to an almost integral action within the regulator, which implies a minimization of $S(s)$ and ensures a good precision in steady state. The pulsation ω_1 for which the range intersects the 0 dB axis can be interpreted as the minimum bandwidth required for the control. The M_s value limits the maximum, in high frequencies, of the frequency response of the sensitivity function $S(s)$ [8].

To limit the function $K.S(s)$, we use $W_2(s)$ and ensure system stability when there is uncertainty, $W_2(s)$ must satisfy the following condition [9][10]:

$$\|W_2 \cdot K \cdot S\|_\infty \leq \gamma \Leftrightarrow \forall \omega \in R \quad |KS(j\omega)| \leq \frac{\gamma}{|W_2(j\omega)|} \quad (26)$$

$$W_2(s) : \text{ written in the form: } W_2 = \frac{s + \omega_h/M_u}{s \cdot \varepsilon_{us} + \omega_h}$$

The choice of ε_{us} at a low value ensures the attenuation of $K.S(s)$ at high frequencies and consequently leads to the rejection of measurement errors and the limitation of the control energy. The pulsation ω_h limits the amplification range of the measurement noises. This pulsation is chosen sufficiently far from the desired proper pulsation for closed-loop control. The value of M_u limits the maximum of the frequency response of $K.S(s)$ [8].

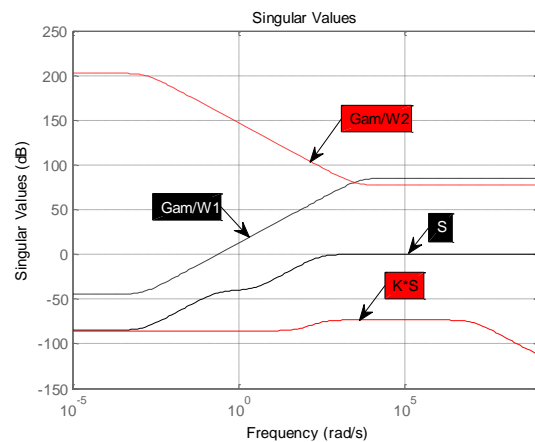


Fig. 6. Frequency response of $S, K \cdot S$ and $\gamma/W_1, \gamma/W_2$ singular values.

The range on $S.G(s)$ depends on the two filters $W_1(s)$ and $W_3(s)$ to ensure the stability of our system it is [9], [10]:

$$\|W_1 \cdot S \cdot G \cdot W_3\|_\infty \leq \gamma \Leftrightarrow \forall \omega \in R \quad |SG(j\omega)| \leq \frac{\gamma}{|W_1 \cdot W_3(j\omega)|} \quad (27)$$

In some cases, it is sufficient to take $W_3(s)$ constant, which allows to adjust attenuation at low frequencies. However, $W_3(s)$ also allows to modify the behavior of $S.G(s)$ in medium frequencies, which proves obtaining a correct transient behavior in presence of disturbance.

The range on $S.G(s)$, if the filters $W_1(s), W_2(s), W_3(s)$ were chosen according to the preceding considerations, are evidently determined [9], [10].

$$\|W_2 \cdot K \cdot S \cdot G \cdot W_3\|_\infty \leq \gamma \Leftrightarrow \forall \omega \in R \quad |KSG(j\omega)| \leq \frac{\gamma}{|T(j\omega)|} \leq \frac{\gamma}{|W_2 \cdot W_3(j\omega)|} \quad (28)$$

However, in some cases it may be preferable to adjust by $W_3(s)$ the template on $KSG(s)$ rather than range on $SG(s)$, for example to satisfy an attenuation template ensuring robustness to neglected dynamics [9].

Weighting functions are not necessarily first order functions. They can be constant or order superior according to the constraints of the specifications and the needs of the designer for the realization of the controller.

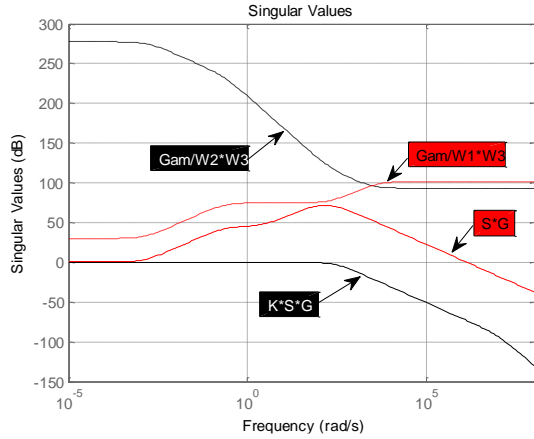


Fig. 7. Frequency response of (S*G, K*S*G) and $\gamma/W_2W_3, \frac{\gamma}{W_1W_3}$ singular values.

Figs. 6 and 7 illustrate the appearance of the sensitivity function S and complementary sensitivity $T = S.G$. These functions are given for the nominal system (without uncertainties), and for the system with uncertainties given by the curves of the inverse of the weighting function of $\gamma/W_1, \gamma/W_2$. Figs. 6, 7 show that the infinite norm of condition (16) is lower than γ . The sensitivity function S shows a very low gain (-50 dB to 1 rd /s) which implies a very low static error and a good rejection of disturbances.

The complementary sensitivity function T shows a very low gain in high frequencies (-410dB to 10000rd/s) which ensures a very good attenuation of noise.

Fig. 8 presents the proposed control scheme for a DFIG using H_∞ controller

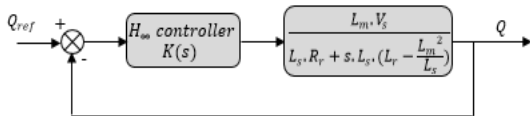


Fig. 8. Control loop by controller H_∞ .

The transfer function corresponding to the nominal parameters of the DFIG is given by:

$$G_p(s) = \frac{G_{0,p}}{1+T_p.s} = \frac{1.8674e+04}{1+0.0141.s} \quad (29)$$

$$W_1 = \begin{bmatrix} \frac{s/M_s + \omega_1}{s + \omega_1.\varepsilon} & 0 \\ 0 & \frac{s/M_s + \omega_1}{s + \omega_1.\varepsilon} \end{bmatrix} \quad (30)$$

$$W_2 = \begin{bmatrix} \frac{s + \omega_h/M_u}{s.\varepsilon_{us} + \omega_h} & 0 \\ 0 & \frac{s + \omega_h/M_u}{s.\varepsilon_{us} + \omega_h} \end{bmatrix} \quad (31)$$

$$W_3 = \begin{bmatrix} 0.42 & 0 \\ 0 & 0.021 \end{bmatrix} \quad (32)$$

We obtain $\gamma = 0.4249$, and the controller H_∞ of the reactive power of order 3 whose transfer function is given as follows:

$$K_Q(s) = \frac{1.63e04 s^2 + 5.109e07 s + 3.53e09}{s^3 + 1.094e06 s^2 + 3.341e09 s + 4.469e06} \quad (33)$$

We obtain $\gamma = 0.5067$, and the controller H_∞ of the active power of order 3 whose transfer function is given as follows:

$$K_P(s) = \frac{7.094 s^2 + 1.41e05 s + 9.928e06}{s^3 + 1.775e05 s^2 + 3.141e09 s + 3.141e09} \quad (34)$$

To improve the performance of our system, we can solve the problem of the parameter variations and disturbances on the control, which have consequences on system performances and stability. In this part, we will focus on the replacement of the classical PI regulator by a fuzzy controller where the regulator adapts to the operating conditions of the system. As mentioned in Fig. 3.

4. FUZZY LOGIC CONTROL

Fuzzy logic allows doing the link between numerical and linguistic modeling, which has allowed spectacular industrial developments from very simple algorithms for the translation of symbolic knowledge into a digital entity and vice versa. Fuzzy set theory has also given rise to an original treatment of uncertainty, based on the idea of order, which formalizes the treatment of partial ignorance and inconsistency in information systems advances [13], [14], [17], and [19].

Fuzzy sets have an impact on automatic classification techniques, and have contributed to some renewal of existing approaches to decision support.

4.1. Structure of a Fuzzy Regulator with Five Assemblies

The design of a fuzzy system consists of three main steps: converting inputs to fuzzy values, evaluating the rules, and converting the result of the rules to a digital output value. The first step is fuzzification uses; to transform the physical quantities (entries) into linguistic value (sub-set fuzzy). The second step is the inference module, which consists of two blocks, the inference engine and the rule base. Finally, the step of defuzzification which makes it possible to infer a net value (precise) [16].

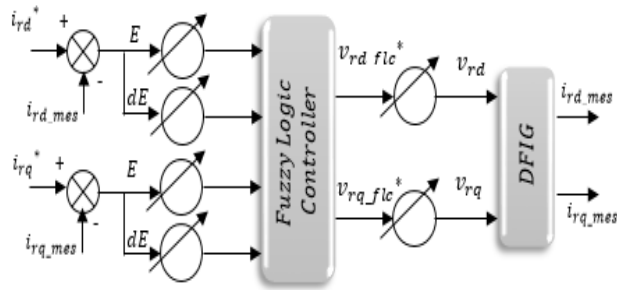


Fig. 9. The proposed fuzzy controller to regulate the active and reactive power of DFIG through the control of i_{rq}, i_{rd} .

As illustrated in Fig. 9, we note: E : The error, it is defined by:

$$\begin{cases} E_{rd}(k) = i_{rd}^*(k) - i_{rd}(k) \\ E_{rq}(k) = i_{rq}^*(k) - i_{rq}(k) \end{cases} \quad (35)$$

dE : The derivative of the error, it is approximated by:

$$dE_{r-d,q}(k) = \frac{E_{r-d,q}(k) - E_{r-d,q}(k-1)}{T_I} \quad (36)$$

T_I : The sampling period.

The output of the regulator is given by:

$$\begin{cases} v_{rd_flc}^*(k) = v_{rd_flc}^*(k-1) + dv_{rd_flc}^*(k) \\ v_{rq_flc}^*(k) = v_{rq_flc}^*(k-1) + dv_{rq_flc}^*(k) \end{cases} \quad (37)$$

$$\begin{cases} v_{rd}(k) = v_{rd_fl}^*(k) - (g\omega_s l_r \cdot \sigma \cdot i_{qr}) \\ v_{rq}(k) = v_{rq_fl}^*(k) + g\omega_s l_r \cdot \sigma \cdot i_{dr} + g \cdot \frac{l_m v_s}{l_s} \end{cases} \quad (38)$$

4.2. Fuzzification

It consists of transforming the physical quantities into linguistic variables (fuzzy variables) represented by the fuzzy sets of the variables $E_{rd}(k)$, $dE_{rd}(k)$, and $v_{rd_flc}^*(k)$ and their membership functions which can be processed by the mechanism of inference. We have chosen to each variable the triangular shapes as shown in the following Figs [13], [14], [17]:

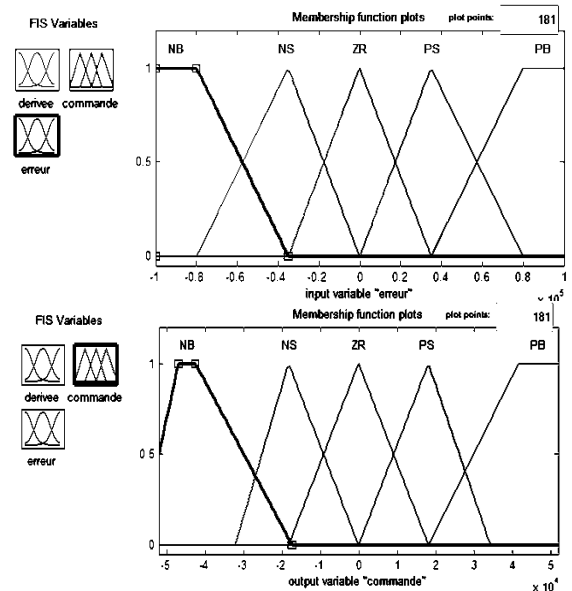
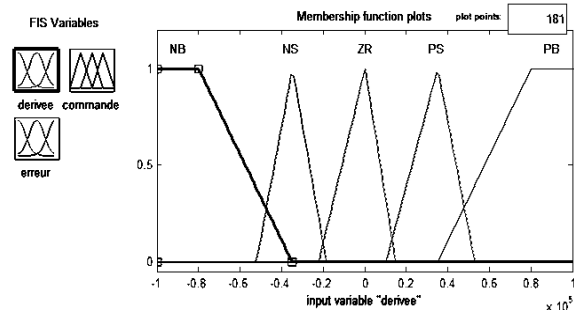


Fig. 10. Input and output membership functions of current controller.

The linguistic variables are noted as follows: NB for negative big, NS for negative small, EZ for approximately zero, PS for positive small, and PG for positive big.

4.3. The Base Rules

It is the rule collection that binds fuzzy input and output variables, they have the form: "if ...then", they can be written verbatim using inputs and outputs and they are given by experts in a direct numerical manner or by terms or linguistic variables through membership functions [16], [19].

4.4. Inference

It calculates the fuzzy set associated with the command and is done by fuzzy inference operations and rule aggregation. Table 1 illustrates the inference matrix of the fuzzy regulator at five sets [14].

Table 1. Rule bases of current fuzzy controller.

dE/E	NB	NS	EZ	PS	PB
NB	NB	NB	NB	NS	EZ
NS	NB	NS	NS	EZ	PS
EZ	NB	NS	EZ	PS	PB
PS	NS	EZ	PS	PS	PB
PB	EZ	PS	PB	PB	PB

There are three main and common methods; Max-Min, Max-Product and Sum-Product, and the method we used in this work is the Max-Min method (Mamdani implication).

4.5. Defuzzification

This step consists of performing the inverse operation of the fuzzification, which is to say, obtaining a physical value of the output from the surface obtained. Several methods of defuzzification exist, we are interested in the center method of gravity because of its simplicity of calculations and its unique output [13].

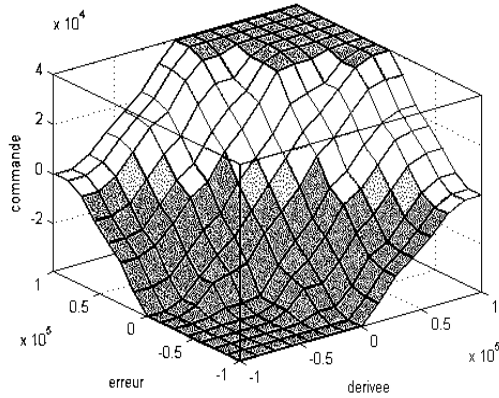


Fig. 11. Fuzzy rule surface for the proposed fuzzy controller with five assemblies.

Three-dimensional representation of the function $dCi_{rq} = f(E, dE)$ in normalized coordinates is shown in Fig. 11 and the surface related to the fuzzy controller is smooth and has good symmetry.

Fig. 12 gives the global control scheme for a DFIG based wind turbine with the H ∞ Fuzzy Logic controller.

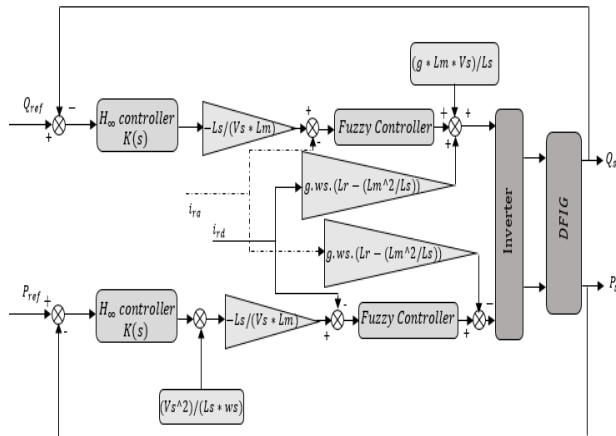


Fig. 12. General diagram of control the stator powers (active and reactive) by H ∞ Fuzzy Logic Controller.

5. SIMULATION RESULTS

The proposed DFIG control has been evaluated via simulation tests through MATLAB/Simulink. The nominal power of DFIG used in the simulation is 1.5 MW.

The simulation of wind system is based on DFIG with two controllers; H ∞ PI and H ∞ Fuzzy. These simulations are performed to compare these regulators in terms of trajectory tracking (reactive and active power), sensitivity to disturbances and robustness with respect to the variation of DFIG parameters.

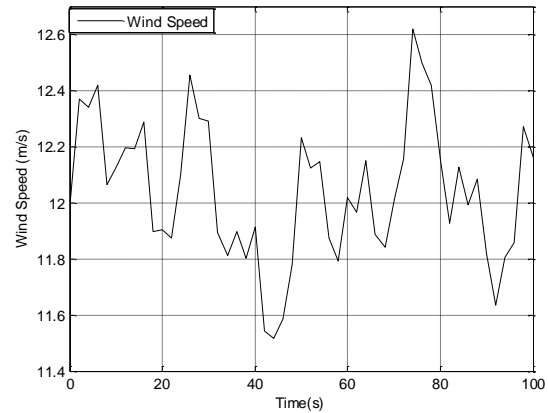


Fig. 13. The profile of wind speed.

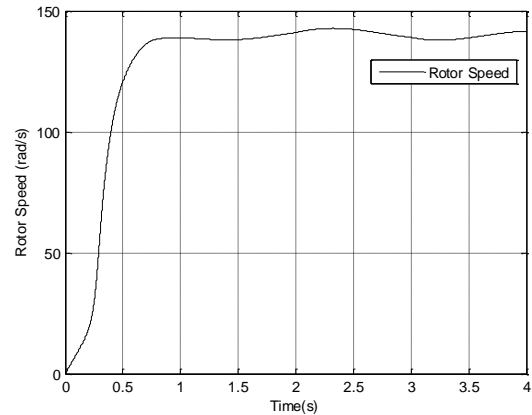


Fig. 14. Rotor speed of DFIG.

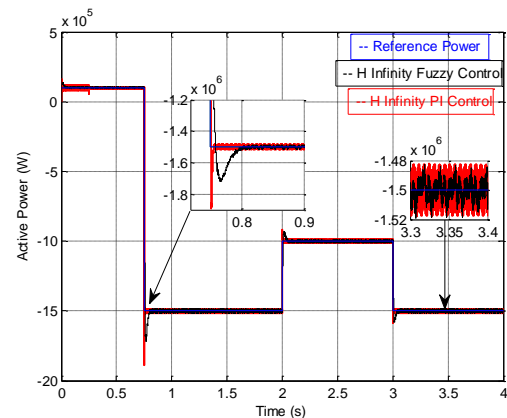


Fig. 15. Dynamics of tracking active power reference, with H ∞ PI and H ∞ Fuzzy controllers.

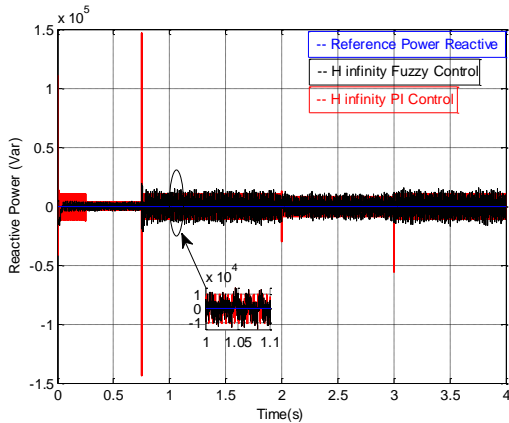


Fig. 16. Dynamics of tracking reactive power reference, with H ∞ PI and H ∞ Fuzzy controllers.

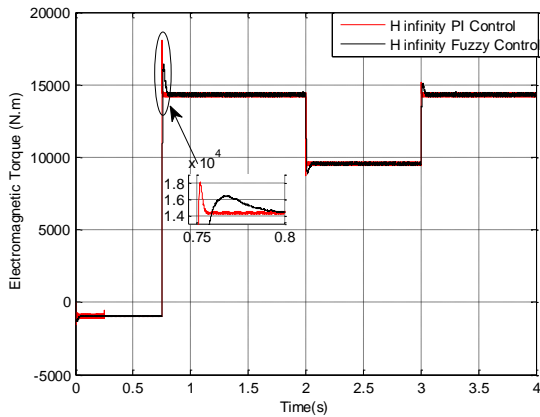


Fig. 17. Electromagnetic Torque.

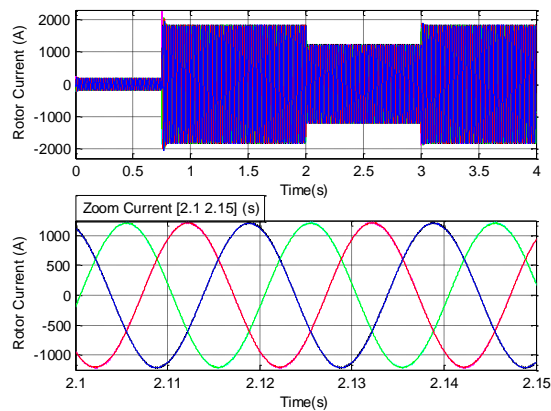


Fig. 18. Stator current.

Figs. 15 and 16 present powers dynamics, for example; the active power reference is selected as time-varying trajectory while the reactive power reference is imposed null to guarantee a nominal stator power factor and the robustness against the machine's parameters variations.

From these results, we can observe the difference between the reference power and the measured one that

is negligible in the cases of corrector H ∞ Fuzzy, but it is important in the case of the corrector H ∞ PI. It is possible to explain that the H ∞ PI controller has no mechanism for ensuring the cancellation of the static error as in the H ∞ fuzzy. In addition, for the transient regime, and for both controller, a peak in active and reactive power dynamics is provoked, such as a high amplitude peak appears in the stator active and reactive power controlled by H ∞ PI at $t=0.75s, 2s$ and $3s$, caused by active power reference changing, while a less peak amplitude for the active and reactive power controlled by H ∞ Fuzzy.

As the conclusion for this test, the H ∞ Fuzzy controller shows a good tracking performance even in presence of variable power reference.

5.1. Robustness Test

The robustness test consists of varying the parameters of the DFIG electric parameters used; these parameters are subject to variations driven by different physical phenomena (saturation of the inductances, heating of the resistors, etc.).

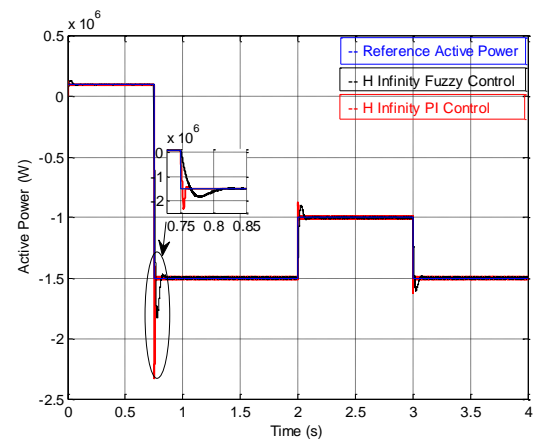


Fig. 19. Effect of variation (100%) of rotor resistance on active power.

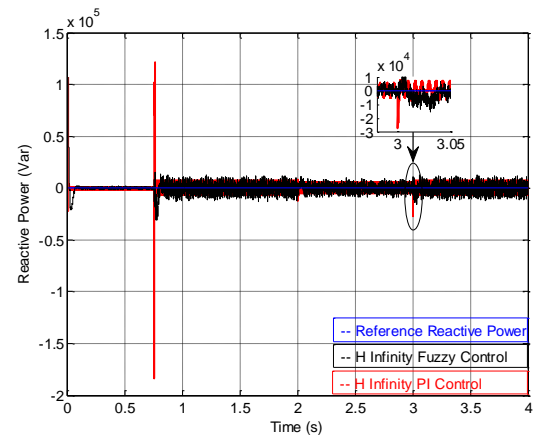


Fig. 20. Effect of variation (100%) of rotor resistance on reactive power.

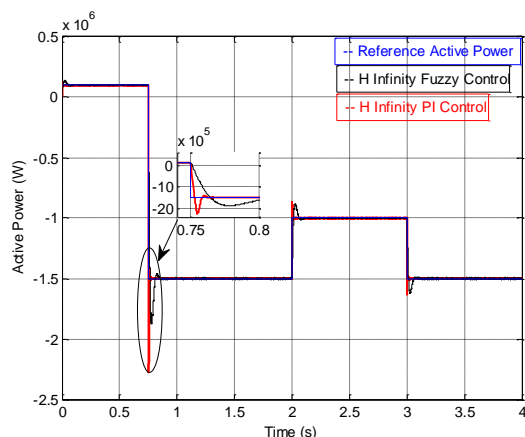


Fig. 21. Effect of variation (50%) of rotor inductance L_r on active power, with H_∞ PI and H_∞ Fuzzy controllers.

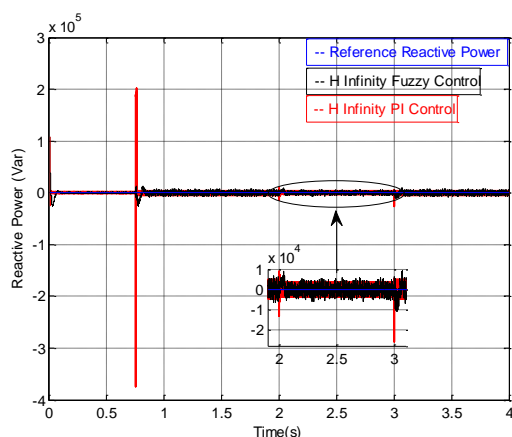


Fig. 22. Effect of variation (50%) of rotor inductance L_r on reactive power, with H_∞ PI and H_∞ Fuzzy controllers.

Parameter variations (resistance, inductance) significantly increase the deviation and response time of H_∞ PI controller, as illustrated in Figs. 19, 20, we note that the variation of the rotor resistance causes a difference which exceeds twice the active power and 3 times the reactive power for a similar test without variation of the resistance for the corrector H_∞ PI. The H_∞ Fuzzy controller has good performance for this test (almost invisible effect). In addition, H_∞ PI controller has a better performance for variation of the inductances, two times better than normal condition, while the proposed controller has no effect to this disturbance.

6. CONCLUSION

This paper enables us to compare the performance of two controllers which are applied to wind turbine system based on DFIG: H_∞ PI controller based on the minimization of the H_∞ standard, using frequency concepts and H_∞ Fuzzy regulator to improve the performance and robustness of H_∞ PI controller.

The purpose of these controllers is to control the active and reactive power exchange between the stator of the DFIG and the grid by modifying the amplitude and the frequency of the rotor voltages, also the performances of the regulators were evaluated by several tests of simulations. For this purpose, the differences between the two regulators are significant with respect to the set-point tracking, although the H_∞ PI regulator seems to have a bad precision which can be improved by a judicious choice of the template on the sensitivity function.

For robustness, the controller based on H_∞ Fuzzy presents high performances to parameter variations and noise rejection; these tests have shown the effectiveness of the H_∞ Fuzzy controller compared to the H_∞ PI regulator.

REFERENCES

- [1] S. Abdelmalek, H. Belmili, L. Barazane, L. Abdelkader, "A New Robust H_∞ Control Power", *International Conference on Control, Engineering & Information Technology (CEIT'14) Proceedings - Copyright IPCO-2014*, pp.123-128 ISSN 2356-5608, 2014.
- [2] M. El azaoui, H. Mahmoudi and C. Ed-Dahmani, "Backstepping control of a doubly fed induction generator integrated to wind power system", *2nd International Conference on Electrical and Information Technologies IEEE*, 2016.
- [3] M. Doumi, A.G. Aissaoui, A. Tahour, M. Abid, and K. Tahir, "Nonlinear Backstepping Control of a Double-Fed Induction Generator", *4th International Conference on Renewable Energy Research and Applications*, Palermo, Italy; 2015.
- [4] C. Busca, A-I. Stan, T. Stanciu and D. Ioan Stroe, "Control of Permanent Magnet Synchronous Generator for Large Wind Turbines", *IEEE*, 2010.
- [5] S. Pati, S. Samantray, "Decoupled Control of Active and Reactive Power in A DFIG Based Wind Energy Conversion System with Conventional PI Controllers", *ICCPCT, IEEE* 2014.
- [6] S. Khoete, Y. Manabe, M. Kurimoto, T. Funabashi and Takeyoshi Kato, "Robust H-infinity Control for DFIG to Enhance Transient Stability during Grid Faults", *Proceedings of the World Congress on Engineering and Computer Science 2016*, Vol II WCECS 2016, San Francisco, USA, 2016.
- [7] W., Yun; W., Qiuwei; G., Wenming; G., Mikkell, P. Sidoroff, "H-infinity Robust Current Control for DFIG Based Wind Turbine subject to Grid Voltage Distortions", *Published in: IEEE Transactions on Sustainable Energy*, 2016.
- [8] G. Djamel Eddine, N. Abdellatif, "Commande Robuste H_∞ Optimisée par L'algorithme Génétique Appliquée à La Régulation Automatique d'Excitation des Générateurs Synchrones Puissants (Application sous GUI/MATLAB)", *Revue « Nature & Technologie » janvier 2016*.
- [9] J. Khedri, M. Chaabane, M. Souissi, "Multivariable H_∞ Robust Controller for a Permanent Magnet

- Synchronous Machine (PMSM)**”, *2015 International Journal on Computer Science and Engineering (IJCSE)*, 2015.
- [10] S. Ozana, M. Pies, “**Application of H-infinity Robust Controller on PAC**”, *VSB-Technical University of Ostrava, FEI. Czech Republic*, Octobre 2010.
- [11] A. Hassan; Yehia S. Mohamed, Ali M. Yousefand A. M. Kassem, “**Robust Control Based On H ∞ Approach For A Wind Driven Induction Generator Connected To The Utility Grid**”, *Journal of Engineering Sciences, Assiut University*, Vol. 34, No. 3, pp. 779-797, May 2006.
- [12] P.Gahinet, P.Apkarian, “**Structured H ∞ Synthesis in MA TLAB**”, *Preprints of the 18th IFAC World Congress Milano (Italy) August 28 - September 2, 2011*.
- [13] Abdul Motin Howlader, Naomitsu Urasaki, Atsushi Yona, Tomonobu Senjyu and Ahmed Yousuf Saber “**Design and Implement a Digital H ∞ Robust Controller for a MW-Class PMSG-Based Grid-Interactive Wind Energy Conversion System**”, *Energies 2013*, 6, 2084-2109; doi:10.3390/en6042084.
- [14] H. Karimi, Davijani, A. Sheikholeslami, H. Livani and M. Karimi-Davijani, “**Fuzzy Logic Control of Doubly Fed Induction Generator Wind Turbine**”, *World Applied Sciences Journal*, Vol. 6(4), pp. 499-508, 2009, ISSN 1818-4952.
- [15] N. Chayaopas, W. Assawin chaichote, “**H ∞ Fuzzy Integral Power Control for DFIG Wind Energy System**”, *International Journal of Electrical and Computer Engineering*, Vol: 11, No:5, 2017.
- [16] B.Hamane, M. Benghanem, A.M.Bouzid, A.Belabbes,M.Bouhamida,A.Draou, “**Control for Variable Speed Wind Turbine Driving a Doubly Fed Induction Generator using Fuzzy-PI Control**”, *Elsevier Energy Procedia 18*, pp. 476 – 485, 2012.
- [17] M. El Azzaoui, “**Fuzzy-PI Control of a Doubly Fed Induction Generator-based Wind Power System**”, *International Journal of Automation and Control*, 2017.
- [18] N. Zerzouri and H. Labar, “**Active and Reactive Power Control of a Doubly Fed Induction**”, *International Journal of Power Electronics and Drive System*, Vol. 5, pp. 244-251, October 2014.
- [19] F. Mazouz, S. Belkacem, Y. Harbouche, S. Ouchen And R. Abdessemed “**Fuzzy Control of a Wind System Based on the DFIG**”, *International Conference on Artificial Intelligence in Renewable Energetic Systems*, 2017.